Cellular/Molecular

Morphine and Pain-Related Stimuli Enhance Cell Surface Availability of Somatic δ-Opioid Receptors in Rat Dorsal Root Ganglia

Louis Gendron,[1] Anna Lisa Lucido,[1] Françoise Mennicken,[2] Dajan O'Donnell,[2] Jean-Pierre Vincent,[3] Thomas Stroh,[1] and Alain Beaudet[1]

[1]Department of Neurology and Neurosurgery, Montréal Neurological Institute, McGill University, Montréal, Québec, Canada H3A 2B4, [2]AstraZeneca R&D Montréal, Ville St-Laurent, Québec, Canada H4S 1Z9, and [3]Institut de Pharmacologie Moléculaire et Cellulaire, Unité Mixte de Recherche 6097 du Centre National de la Recherche Scientifique, 06560 Valbonne, France

The present study demonstrates that perikaryal δ-opioid receptors (δORs) in rat dorsal root ganglion (DRG) neurons bind and internalize opioid ligands circulating in the CSF. Using confocal and electron microscopy, we found that prolonged morphine treatment increased the cell surface density of these perikaryal δORs and, by way of consequence, receptor-mediated internalization of the fluorescent deltorphin (DLT) analog ω-Bodipy 576/589 deltorphin-I 5-aminopentylamide (Fluo-DLT) in all three types of DRG neurons (small, medium, and large). In contrast, chronic inflammatory pain induced by the injection of complete Freund's adjuvant (CFA) into one hindpaw selectively increased Fluo-DLT internalization in small and medium-sized DRG neurons ipsilateral to the inflammation. Based on our previous studies in the spinal cord of μ-opioid receptor (μOR) knock-out mice, it may be assumed that the enhanced membrane recruitment of δORs observed after sustained morphine is attributable to stimulation of μORs. However, the selectivity of the effect induced by inflammatory pain suggests that it involves a different mechanism, namely a modality-specific and pain-related activation of C and Aδ fibers. Indeed, stimulation by capsaicin of transient receptor potential vanilloid 1 receptors, which are selectively expressed by small diameter ($< 600\ \mu m^2$) DRG neurons, increased Fluo-DLT internalization exclusively in this cell population. The present results, therefore, demonstrate that DRG neurons express perikaryal δORs accessible to CSF-circulating ligands and that the density and, hence, presumably also the responsiveness, of these receptors may be modulated by both pain-related stimuli and sustained exposure to μOR agonists.

Key words: **δ-opioid receptor; deltorphin; dorsal root ganglia; targeting; chronic inflammation; receptor internalization; fluorescent ligand**

Introduction

Opioids exert their effects by activating one of three subtypes of G-protein-coupled receptors, namely μ (μORs), δ (δORs), and κ (κORs) opioid receptors (for review, see Kieffer, 1999). Opioids acting at the μORs, including morphine, are the most effective of clinically available analgesic drugs. However, they also give rise to several unwanted side effects, such as respiratory depression, constipation, and nausea (Colpaert, 1996; Kreek, 1996). Compounds activating δORs have lower analgesic potency than their μOR-selective counterparts, but they produce only minimal side effects and they do not induce tolerance with prolonged administration (Porreca et al., 1984; May et al., 1989; Sheldon et al., 1990; Szeto et al., 1999; Petrillo et al., 2003), which makes them an attractive alternative to the use of μOR agonists for the treatment of chronic pain.

The limited analgesic potency of δOR-selective agonists may be because of the fact that at steady state only a small proportion of δORs are present on the plasma membrane of neurons, the majority being retained in the cytoplasm (Stewart and Hammond, 1994; Cheng et al., 1995, 1997; Elde et al., 1995; Zhang et al., 1998b; Cahill et al., 2001). However, under certain experimental conditions, intracellular δORs may be recruited to the cell surface, thereby enhancing the pharmacological efficacy of δOR agonists. Thus, in cultured cortical neurons, as well as in neurons of the superficial dorsal horn of the rat spinal cord *in vivo*, prolonged morphine treatment leads to an increase in the density of δORs on dendritic plasma membranes (Cahill et al., 2001). In the spinal cord, this increase in δOR cell surface density was correlated with enhanced antinociceptive potency of intrathecally administered deltorphin (DLT), a δOR-selective agonist (Cahill et al., 2001; Morinville et al., 2003). It also was abolished in μOR knock-out (KO) mice, indicating that it was dependent on the

Received Aug. 24, 2005; revised Nov. 22, 2005; accepted Nov. 23, 2005.

This work was supported by Grant MOP-38014 from the Canadian Institutes of Health Research (CIHR) to A.B. and by grants from AstraZeneca Canada. L.G. was funded by Fellowship MFE-63497 from the CIHR. We are grateful to Mariette Lavallée and Clélia Tommi for expert technical assistance and to Claude Roberge for her help with the design of real-time PCR primers.

Correspondence should be addressed to Dr. Alain Beaudet, Department of Neurology and Neurosurgery, Montreal Neurological Institute, Room 896, 3801 University Street., Montréal, Québec, Canada H3A 2B4. E-mail: alain.beaudet@mcgill.ca.

DOI:10.1523/JNEUROSCI.3598-05.2006

 0270-6474/06/260953-10$15.00/0

stimulation of μORs (Morinville et al., 2003). Likewise, prolonged exposure of periaqueductal gray slices to morphine was found to significantly increase the δOR-mediated presynaptic inhibition of GABAergic currents, presumably through increased recruitment of δORs (Hack et al., 2005).

Stimuli other than μOR activation have been reported to enhance recruitment of δORs to neuronal plasma membranes. Thus, in cultured dorsal root ganglion (DRG) neurons, as well as in PC12 cells, plasma membrane insertion of δORs was observed after neuronal depolarization with KCl (Bao et al., 2003; Kim and von Zastrow, 2003). In the spinal cord, we demonstrated, using electron microscopy and an original *in vivo* fluorescent internalization assay, that chronic inflammation induced by injection of complete Freund's adjuvant (CFA) in the hindpaw increased the cell surface density of δORs bilaterally throughout the lumbar segments (Cahill et al., 2003; Gendron et al., 2005). This increase, in turn, translated into an enhancement of the antinociceptive properties of intrathecally administered δOR agonists (our unpublished observations).

In this context, the aim of the present study was twofold: (1) to determine whether prolonged treatment with morphine or CFA-induced chronic inflammatory pain affected the trafficking of δORs in DRG neurons and (2) to explore the mechanisms underlying these effects.

Parts of this paper have been published previously (Gendron et al., 2004).

Materials and Methods

Animals. All experiments were performed in adult male Sprague Dawley rats (220–280 g; Charles River, Quebec, Canada), maintained on a 12 h light/dark cycle. Experiments were approved by local animal care committees of McGill University (Montreal, Quebec, Canada) and AstraZeneca R&D (St-Constant, Quebec, Canada), and were in accordance with policies and directives of the Canadian Council on Animal Care.

Prolonged morphine treatment. Rats received subcutaneous injections of increasing doses of morphine sulfate (Sabex, Boucherville, Quebec, Canada) every 12 h for 24 h (using doses of 5 and 8 mg/kg, respectively) or 48 h (using doses of 5, 8, 10, and 15 mg/kg, respectively), as described previously (Cahill et al., 2001). The drug was diluted in aqueous 0.9% NaCl solution (saline) from a 50 mg/ml stock solution. Control rats were injected with equivalent volumes of saline alone. *In vivo* δOR internalization assays or perfusion fixation for electron microscopy were performed 12 h after the last morphine or saline injection.

Induction of chronic inflammation. Chronic inflammatory pain was induced by a single subcutaneous injection of 100 μl CFA (Calbiochem, La Jolla, CA) in the plantar surface of the left hindpaw of rats under isoflurane anesthesia. Control rats were left untreated (naive). *In vivo* δOR internalization assays were performed 48 or 72 h after CFA injection, as described below.

Treatment with colchicine. To test whether ω-Bodipy 576/589 deltorphin-I 5-aminopentylamide (Fluo-DLT) was transported axonally, *in vivo* internalization experiments were repeated in rats ($n = 3$) injected intrathecally with a saline solution (30 μl) containing 0.2 mg colchicine 16 h earlier (Hinkley and Green, 1971). Control rats ($n = 3$) were injected intrathecally with saline.

Treatment with capsaicin. To determine whether selective activation of C fibers would affect the cell surface density of δORs in the DRG, 10 μl of a 0.5% capsaicin solution (0.5% capsaicin w/v in 20% ethanol and 7% Tween 80) was injected in the plantar surface of the left hindpaw of rats ($n = 3$) under brief halothane anesthesia. *In vivo* δOR internalization assays were performed 1 h after capsaicin injection, as described below.

Light microscopic δOR immunostaining. To determine the distribution of δOR-immunoreactive ganglion cells in the lumbar DRG, naive rats were killed by intra-aortic arch perfusion with 4% paraformaldehyde (PFA) in 0.1 M phosphate buffer (PB; pH 7.4). DRGs (L4–L5) were dissected and left overnight in 30% sucrose, snap frozen in isopentane at −45°C, and stored at −80°C until sectioning. Twenty-micrometer-thick sections were cut on a cryostat and mounted onto chrom/alum gelatin-coated microscope slides. Sections were rinsed with 3% H_2O_2 diluted in 0.1 M PB for 30 min. They were then preincubated with 3% normal goat serum (NGS; Bio/Can Scientific, Mississauga, Ontario, Canada) in 0.1 M PB for 30 min and incubated overnight at 4°C with δOR antiserum (Ab1560, lot numbers 21100532 or 23010452A; Chemicon International, Temecula, CA) diluted at 4 μg/ml in 0.1 M TBS containing 0.5% NGS. Sections were rinsed with 0.1 M TBS containing 1% NGS and incubated for 45 min with biotinylated goat-anti-rabbit antibody (Vector Laboratories, Burlingame, CA) diluted at 4 μg/ml in 0.1 M TBS. Sections were then rinsed with 0.1 M TBS, incubated with avidin-biotin complex (Vectastain Elite Standard; Vector Laboratories) for 30 min, and reacted for 6 min with 1 mg/ml of DAB-Ni in 0.1 M Tris, pH 7.4, containing $NiCl_2$ and H_2O_2. They were then rinsed in buffer, dehydrated with increasing concentrations of ethanol, cleared with a xylene substitute (Neo-Clear clarification; Cedarlane Laboratories, Hornby, Ontario, Canada), and examined with a Leitz (Wetzlar, Germany) Aristoplan microscope.

β-Tubulin immunostaining. In rats treated with colchicine to impede axonal transport, the efficacy of colchicine injection was verified (16 h after injection) by assessing the integrity of microtubules using β-tubulin immunostaining. Sections (20 μm) from DRGs exposed to intrathecal Fluo-DLT and perfusion-fixed, as described below, were rinsed in 0.1 M TBS, pH 7.4, for 1 h, after which nonspecific sites were blocked with a solution of 1% BSA in 0.1 M TBS. Sections were then incubated for 1 h at room temperature with an FITC-conjugated anti-β-tubulin antibody (Sigma, St. Louis, MO) diluted 1:100 in 1% BSA/0.1 M TBS, and washed twice with 0.1 M TBS. Sections were visualized using a Zeiss (Toronto, Ontario, Canada) confocal laser scanning microscope (LSM 510), equipped with an inverted microscope (oil-immersion objectives, 25×, 40×, and 63×) and a argon/krypton laser with an excitation wavelength of 488 nm.

In vivo *δOR internalization assay.* To assess the cell surface availability of δORs in dorsal root ganglia (L4–L5), naive rats ($n = 4$), rats treated every 12 h for 48 h with saline ($n = 3$) or morphine (using doses of 5, 8, 10, and 15 mg/kg, respectively; $n = 3$), rats injected with CFA 48 h ($n = 3$) or 72 h earlier ($n = 3$), rats injected with colchicine 16 h earlier ($n = 3$), and rats treated with capsaicin 1 h earlier ($n = 3$) were injected intrathecally with Fluo-DLT, as described previously (Morinville et al., 2004). Briefly, animals were anesthetized with sodium pentobarbital (Somnotol; MTC Pharmaceuticals, Cambridge, Ontario, Canada; 6.5 mg/100 g of body weight) and injected with 0.8 nmol of Fluo-DLT diluted in 30 μl of saline via a lumbar puncture at the L5–L6 intervertebral space. Twenty minutes after injection of the fluorescent ligand, rats were killed by intra-aortic arch perfusion of, in succession, 500 ml of 4% PFA in 0.1 M PB, pH 7.4, at 4°C, and 100 ml each of 10, 20, and 30% sucrose in 0.2 M PB, pH 7.4. Lumbar DRGs (L4–L5) were snap frozen in isopentane at −45°C and stored at −80°C until sectioning. Tissues were sectioned on a cryostat at a thickness of 20 μm and thaw-mounted onto chrome alum/gelatin-coated slides (without coverslipping).

Neurons having specifically bound and internalized Fluo-DLT (characterized by the presence of intracytoplasmic fluorescent puncta) were visualized using a Zeiss LSM 510 confocal laser scanning microscope equipped with an inverted microscope (oil-immersion objectives, 25×, 40×, and 63×) and an He/Ne laser with an excitation wavelength of 543 nm. To test for labeling specificity, additional rats ($n = 2$) were injected with 1.6 μmol of naloxone, subcutaneously, 10 min before the intrathecal administration of a mixture of Fluo-DLT (0.8 nmol) and naloxone (1.6 μmol).

Quantification of Fluo-DLT labeling. To quantify the amount of internalized Fluo-DLT in each experimental condition, fluorescence densities were measured over individual labeled cells using computer-assisted microdensitometry. For each animal, 10 representative images (from two DRGs) were acquired. In animals treated unilaterally with CFA (100 μl) or capsaicin (10 μl), 10 representative images were acquired on the side contralateral and 10 additional images on the side ipsilateral to the injected paw. All images were acquired using the same parameters [25× objective; zoom value, 1; detector gain, 955; amplificator (amp) offset, −0.1; amp gain, 1]. These parameters were chosen because they

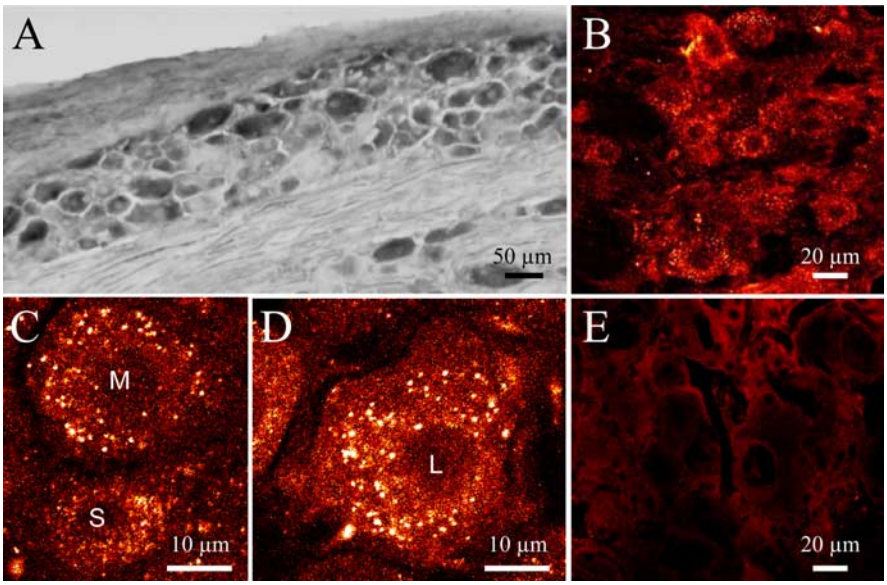

Figure 1. Expression and functionality of δORs in lumbar DRGs. ***A***, DAB immunostaining of DRGs reveals that 40–50% of cells express δORs. ***B***, When injected intrathecally, Fluo-DLT is rapidly internalized by the same proportion of DRG neurons (40–50%), suggesting that most cells expressing δORs have the capacity to bind and internalize Fluo-DLT. ***C***, ***D***, In all three cell types [small (S), medium (M), and large (L)], Fluo-DLT forms endosome-like fluorescent clusters, which pervade the cytoplasm. ***E***, Coinjection of Fluo-DLT with 1.6 μmol of the nonselective opioid antagonist naloxone completely abolishes Fluo-DLT internalization, demonstrating that the fluorescent labeling is specific and mediated by an opioid receptor.

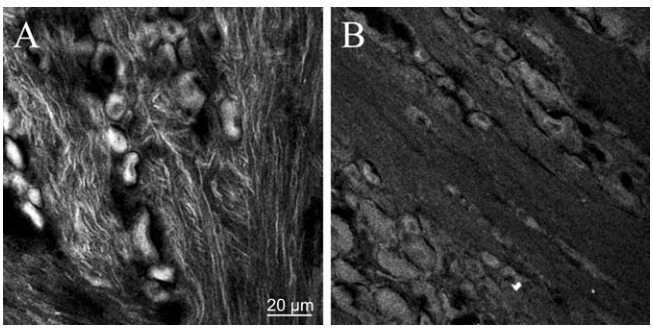

Figure 2. Effect of intrathecal colchicine on β-tubulin immunostaining in lumbar DRGs. Rats injected intrathecally with saline (***A***) or 0.2 mg of colchicine (***B***) were injected intrathecally 16 h later with 0.8 nmol of Fluo-DLT (see Table 1) and processed for confocal microscopic analysis of lumbar DRGs. Some DRG sections (20 μm) were labeled with anti-β-tubulin-FITC to assess the effect of colchicine on microtubules (polymerized tubulin). ***A***, In DRG axons from saline-injected rats, microtubules are clearly delineated by β-tubulin immunostaining. ***B***, In animals treated for 16 h with colchicine, β-tubulin immunoreactivity is diffuse and microtubule-like structures are no longer evident. Images are representative of two independent experiments.

prevented any saturation of the fluorescent signal. Images acquired with the 25× objective were converted to a grayscale using the Zeiss LSM 5 image browser, which attributed to each pixel a single value of intensity ranging from 0 to 255. Using the thresholding function of NIH ImageJ software, we then determined the background fluorescence intensity value (i.e., the density of fluorescence measured in unlabeled cells) as being 30. The fluorescence density (i.e., mean fluorescence intensity per unit surface area minus the background value) was finally calculated for each labeled cell profile, including the nucleus. The surface area of each labeled cell profile was also measured (μm^2) and labeled neurons were subdivided according to their size (small, $<600\ \mu m^2$; medium, from 600 μm^2 to 1200 μm^2; large, $>1200\ \mu m^2$). Only profiles in which the nucleus was clearly visible were included in the analyses to minimize errors in the determination of both fluorescence density and surface area. Cellular fluorescence density values of all animals within a group were then pooled and averaged. Means were expressed as levels of internalized Fluo-DLT (in arbitrary units) ± SEM. Calculations and statistical analyses were performed using Microsoft (Redmond, WA) Excel 2000, GraphPad (San Diego, CA) Prism 3.0, and SigmaPlot 2001 (Systat Software, Point Richmond, CA).

Real-time reverse transcriptase-PCR analysis. Dorsal root ganglia (L4–L5) were removed from animals treated either with CFA (100 μl in the left hindpaw) or with morphine (doses of 5, 8, 10, and 15 mg/kg respectively, given every 12 h over 48 h). For CFA-treated animals, DRGs from ipsilateral and contralateral sides were pooled in two separate groups. Tissue samples were processed for RNA extraction using the SV Total RNA Isolation System (Promega, Madison, WI). Amplification of δOR mRNA was achieved using the one-step QuantiTect SYBR Green reverse transcriptase (RT)-PCR kit (Qiagen, Mississauga, Ontario, Canada), as recommended by the supplier. Briefly, 60 ng of template RNA was mixed on ice with 12.5 pmol of both sense (position 306 in exon 1, 5′-TGCTCGTCATGTTTGGAATCGTC-3′) and antisense (position 386 in exon 2, 5′-GCCAAGGCCAGATTGAAGATGTAG-3′) primers for the amplification of rat δOR mRNA (length of the amplicon is 79 bp, with a melting temperature of 81.3°C), 12.5 μl of the 2× QuantiTect SYBR Green RT-PCR Master Mix, and 0.25 μl of QuantiTect RT mix in a final reaction volume of 25 μl. Primer pairs were also specifically designed for the amplification of rat glyceraldehyde-3-phosphate dehydrogenase (GAPDH) (5′-TGGTGCCAAAAGGGTCATC-3′ and 5′-CTTCCACGATGCCAAAGTTG-3′ for sense and antisense primers, positions 366 and 541 of exons 6 and 7, respectively), used as internal control (length of the amplicon is 176 bp, with a melting temperature of 85.2°C). One-step, real-time RT-PCR analysis was performed on a RotorGene RG-3000 and data were analyzed with RotorGene 4.6 software (Corbett Research, Montreal Biotech, Montreal, Quebec, Canada). The following parameters were used: reverse transcriptase reaction was performed at 50°C for 30 min, after which the enzymes (Omniscript and Sensiscript reverse transcriptases; Qiagen) were inactivated at 95°C for 15 min. The latter step also served in activating the HotStart Taq DNA polymerase. Amplification was then achieved with 35 cycles of denaturation (15 s at 94°C), annealing (30 s at 54°C), and extension (30 s at 72°C, fluorescence intensity was read at the end of this step). Comparative concentration of δOR mRNA in each sample was determined with RotorGene 4.6 software and Excel 2000, using GAPDH as the housekeeping gene (i.e., the ratio of δOR/GAPDH mRNA fluorescence levels).

Electron microscopic δOR immunostaining. For electron microscopic analysis of immunoreactive δOR distribution in DRGs, saline-injected ($n = 3$) and morphine-injected rats ($n = 3$) were anesthetized with sodium pentobarbital (6.5 mg per 100 g of body weight) and perfused through the aortic arch with 45 ml of heparin (75 U/ml of heparin in 0.9% saline) followed by 50 ml of a mixture of 3.75% acrolein and 2% PFA in 0.1 M PB, pH 7.4, and then by 300 ml of 2% PFA in the same buffer at 45 ml/min. Lumbar DRGs (L4–L5) were removed and postfixed in 2% PFA in 0.1 M PB for 1 h at 4°C. Sections (100 μm thick) were cut using a Vibratome 1000 (Vibratome, St. Louis, MO) and processed for δOR immunogold labeling as described previously. Sections were incubated in 1% sodium borohydride for 30 min and extensively rinsed in 0.1 M PB. They were then cryoprotected for 30 min in a solution consisting of 25% sucrose and 3% glycerol in 0.05 M PB and snap frozen with isopentane (−50°C) followed by liquid nitrogen. After being rapidly thawed in 0.1 M PB, sections were rinsed with TBS and preincubated for 1 h at room temperature in 3% NGS diluted in TBS. They were then incubated for 36 h at 4°C in δOR antiserum (Ab1560, lot numbers 21100532 and 23010452A) diluted to 1 μg/ml in TBS containing 0.5% NGS. Sections

were then rinsed and incubated for 2 h with colloidal gold (1 or 2 nm)-conjugated goat anti-rabbit IgG (1:50; Cedarlane Laboratories) diluted in 0.01 M PBS containing 0.1% gelatin and 0.8% BSA. They were then fixed with 2% glutaraldehyde in 0.01 M PBS and washed with 0.2 M citrate buffer, pH 7.4, after which immunogold particles were silver-intensified for 7 min using an IntenSEM kit (Amersham Biosciences, Baie d'Urfé, Quebec, Canada). Sections were postfixed for 40 min with 2% osmium tetroxide in 0.1 M PB, rinsed, and dehydrated in increasing concentrations of ethanol. They were embedded in Epon 812 resin and cured between plastic coverslips at 60°C for 24 h. Ultrathin sections (80 nm) were collected from the surface of immunoreacted sections and counterstained with lead citrate and uranyl acetate for examination with a JEOL (St-Hubert, Quebec, Canada) 100 CX transmission electron microscope.

For data analysis, negatives were scanned using an AGFA (Mortsel, Belgium) Duoscan T1200 and the number of membrane-associated versus intracellular gold/silver grains was assessed using NeuroLucida software (MicroBrightField, Williston, VT). Because in most cases only a fraction of labeled ganglion cell profiles was visible within a grid square, we restricted grain counts to visible sections of the membrane (membrane-associated grains) and to the surface area underlying this membrane to a distance of 1 μm (intracellular grains). For each portion of cell profile thus analyzed, the ratio of the number of gold/silver grains in direct contact with the plasma membrane over the total number of grains within 1 μm from the plasma membrane was determined and expressed as the percentage of grains at the membrane. Results from 8–10 cell profiles (or portions of cell profiles) per animal were pooled and averaged. Means were expressed as the percentage of grains at the membrane ± SEM. Calculations and statistical analyses were performed using Microsoft Excel 2000, GraphPad Prism 3.0, and SigmaPlot 2001.

DRG primary cell culture and immunocytochemistry for electron microscopy. For DRG cell cultures, two male Sprague Dawley rats were anesthetized with halothane and humanely decapitated. DRGs were then rapidly dissected, placed in warmed culture medium (Ham's F-12 medium supplemented with 3 mM L-glutamine, 1% Pen/Strep, 40 mM D-glucose, and 0.1% fungizone; all from Invitrogen, Burlington, Ontario, Canada), and minced into fine pieces. Minced DRGs were then transferred to Falcon tubes containing filter-sterilized collagenase D (Roche Pharmaceuticals, Laval, Quebec, Canada; 0.25% w/v in DRG medium) and incubated at 37°C for 90 min. Cells were centrifuged at 3000 rpm for 2 min, resuspended in 0.25% trypsin (Invitrogen) in HBSS (Invitrogen), and incubated at 37°C for a minimum of 15 min. Using successively smaller fire-polished Pasteur pipettes, DRGs were triturated until the solution appeared homogeneous. The reaction was stopped by adding an equal volume of the culture medium and the cell suspension was passed through a 70 micron cell strainer. After a brief centrifugation, cells were resuspended into complete DRG medium (culture medium supplemented with 10% FBS and 40 ng/ml of NGF 2.5S; Invitrogen). DRG cells were finally plated onto poly-D-lysine/mouse laminin coated four-well plates and grown at 37°C in a 95% air/5% CO_2 atmosphere. Half of the culture medium was changed every second day. After 6–8 d in culture, cells were left untreated or exposed to 10 μM morphine for 48 h, washed once gently with 0.1 M PB, pH 7.4, and fixed as described below. To assess the effect of membrane depolarization on the targeting of δORs, some wells were treated with 40 mM KCl for 5 min before fixation for immunolabeling.

For δOR immunolabeling, cells were fixed first with a solution of 2% acrolein/2% PFA in 0.1 M PB for 20 min, followed by 2% PFA in 0.1 M PB for 20 min. They were then rinsed in 0.1 M TBS, incubated for 30 min in 3% NGS diluted in 0.1 M TBS containing 0.02% Triton X-100, rinsed with 0.1 M TBS, and incubated for 40–48 h at 4°C in δOR antiserum (Ab1560, lot numbers 21100532 and 23010452A) diluted to 1 μg/ml in 0.1 M TBS supplemented with 0.5% NGS. After a brief rinse with 0.01 M PBS, they were incubated for 10 min in 0.01 M PBS containing gelatin and BSA, followed by colloidal gold (1 or 2 nm)-conjugated goat anti-rabbit IgG (1:50) diluted in 0.01 M PBS containing 0.1% gelatin and 0.8% BSA for 2 h at room temperature. Subsequently, cells were fixed with 2% glutaraldehyde in 0.01 M PBS for 10 min and rinsed with 0.2 M citrate buffer, pH 7.4. Immunogold particles were silver intensified for 7 min using an IntenSEM kit and rapidly rinsed with citrate buffer. Cells were then postfixed for 10 min with 2% osmium tetroxide in 0.1 M PB, rinsed with 0.1 M PB, and dehydrated in graded alcohols. After dehydration, the

Table 1. Internalization of Fluo-DLT in dorsal root ganglia of rats treated intrathecally with colchicine

	Levels of internalized Fluo-DLT (% of saline-injected rats)
Small neurons (<600 μm^2)	108.5 ± 4.0
Medium neurons (from 600 to 1200 μm^2)	91.9 ± 3.5
Large neurons (>1200 μm^2)	87.9 ± 6.0

Data are the mean ± SEM of the fluorescence density of DRG cell profiles from colchicine-treated rats (0.2 mg/30 μl of saline, i.t.) and saline-treated rats (30 μl, i.t.) and are expressed as the levels of internalized Fluo-DLT in colchicine-treated rats as a percentage of saline-injected animals. The density of fluorescence for each individual cell profile was determined by densitometric analysis of confocal images as described in Material and Methods. No significant difference was found when comparing the amount of Fluo-DLT internalized in colchicine-treated versus saline-treated animals ($p = 0.1$, 0.08, and 0.15 for small, medium, and large DRG neurons, respectively; two-tailed unpaired *t* test).

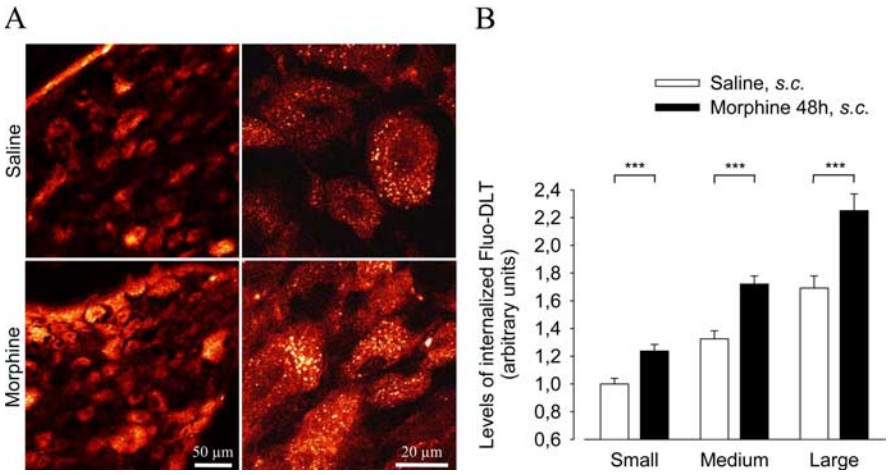

Figure 3. Effect of prolonged morphine treatment on Fluo-DLT internalization in lumbar DRGs. Rats treated subcutaneously for 48 h with either saline or morphine (using doses of 5, 8, 10, and 15 mg/kg respectively, given every 12 h) were injected intrathecally with 0.8 nmol of Fluo-DLT and DRGs were processed for confocal microscopy. ***A***, Red-white glow-scale images of L4–L5 DRGs. Note the higher intensity of Fluo-DLT-induced fluorescence in morphine-treated as compared with saline-injected rats. ***B***, Densitometric analysis of the effect of morphine pretreatment on Fluo-DLT internalization in DRGs. Prolonged morphine treatment significantly increases levels of internalized Fluo-DLT (expressed ± SEM) in all types of DRG neurons (***$p < 0.001$; two-tailed unpaired *t* test).

Table 2. Ratio of δOR/GAPDH mRNA expression in the rat dorsal root ganglia

	Ratio of δOR/GAPDH	*n*
Saline	0.116 ± 0.012	6
MS 24 h	0.167 ± 0.033	4
MS 48 h	0.131 ± 0.012	4
CFA 72 h (ipsi)	0.132 ± 0.018	4
CFA 72 h (contra)	0.134 ± 0.004	3

Data are the mean ± SEM of the ratio of δOR/GAPDH mRNA fluorescence levels in rat dorsal root ganglia after real-time RT-PCR amplification. No significant difference is apparent between any groups ($p > 0.05$; one-way ANOVA followed by Bonferroni's MCT). MS 24 h, Morphine sulfate 24 h (using doses of 5 and 8 mg/kg, respectively, given every 12 h); MS 48 h, morphine sulfate 48 h (using doses of 5, 8, 10, and 15 mg/kg, respectively, given every 12 h); ipsi, side ipsilateral to CFA injection; contra, side contralateral to CFA injection; *n*, number of rats tested in each condition.

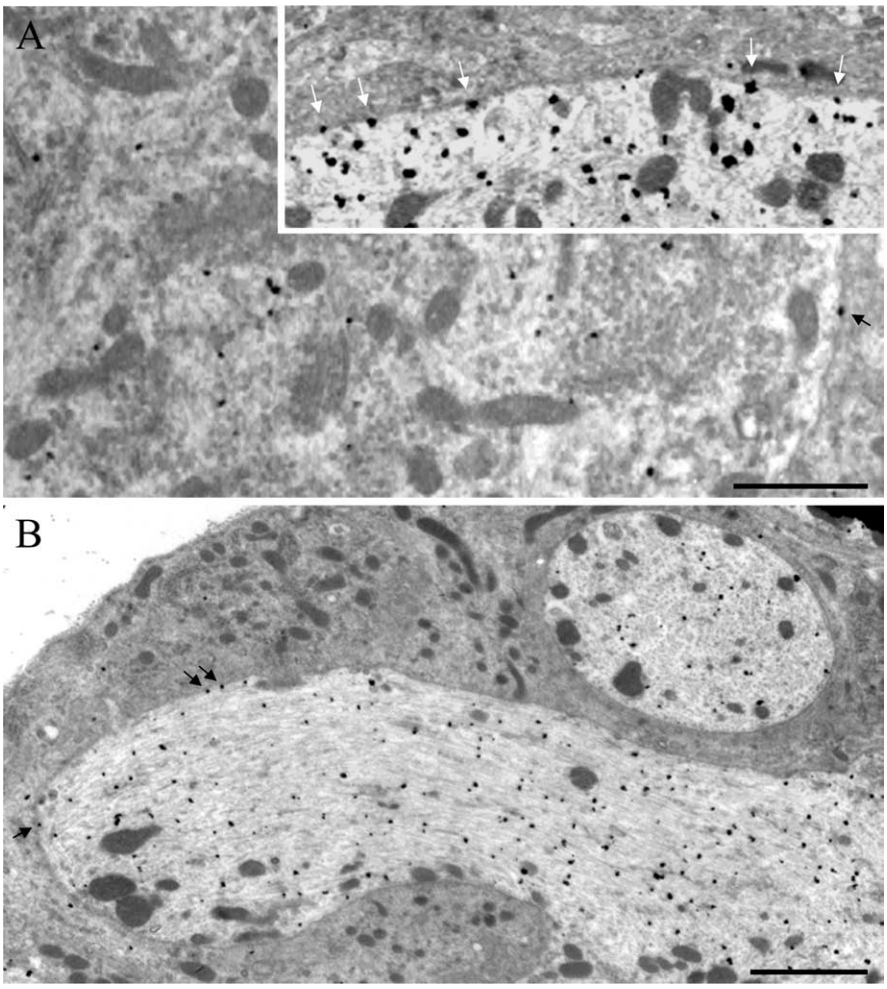

Figure 4. Effect of prolonged morphine treatment on the membrane targeting of δORs in lumbar DRGs. Rats were treated subcutaneously for 48 h with either saline or morphine (using doses of 5, 8, 10, and 15 mg/kg, respectively, given every 12 h), and lumbar DRGs were processed for transmission electron microscopic analysis as described. ***A***, Type A_2 ganglion cells show the highest concentration of δOR immunostaining. In these cells, gold/silver particles (corresponding to immunoreactive δORs) are mainly associated with Nissl bodies and mitochondria but are also found over the plasma membrane (black arrow; inset, white arrows). ***B***, A very high density of gold/silver particles is also observed in the axon hillock, both on the cell membrane (black arrows) and in the cytoplasm. Scale bars: ***A***, 1 μm; ***B***, 2 μm.

cells were infiltrated with Epon 812 resin and allowed to polymerize for 24 h at 60°C. Ultrathin sections (80 nm thick) were collected, counterstained with lead citrate and uranyl acetate, and examined using a JEOL 100CX or a Phillips 410 transmission electron microscope (FEI Systems, Toronto, Ontario, Canada).

For data analysis, negatives were scanned using an AGFA Duoscan T1200 and the number of membrane-associated versus intracellular gold/silver grains was assessed using NeuroLucida software. Because the density of silver/gold grains was considerably lower in cultured than in *ex vivo* preparations, counts of intracellular grains were not restricted to the zone comprised within 1 μm of the cell surface, but included all grains visible within the labeled profile. Hence, for each cell profile analyzed, we established the ratio of the number of gold/silver grains in direct contact with the plasma membrane over the total number of grains within the whole cell profile. In the analysis, 21 control cells, 12 morphine-treated cells, and 8 KCl-stimulated cells were included. Means were expressed as the percentage of grains at the plasma membrane ± SEM obtained from two (for morphine and KCl treatments) to three (for controls) independent experiments. Calculations and statistical analysis were performed using Microsoft Excel 2000, GraphPad Prism 3.0, and SigmaPlot 2001.

Results

Internalization of Fluo-DLT in DRGs

We first assessed the capacity of DRG neurons to specifically bind and internalize intrathecally administered Fluo-DLT. As shown in Figure 1*B*, 20 min after intrathecal injection of 0.8 nmol of Fluo-DLT, fluorescent labeling was observed throughout the cytoplasm of ~40–50% of DRG neurons. This labeling was highly punctate, consistent with endosomal sequestration of the fluorescent ligand (Lee et al., 2002; Morinville et al., 2004). It was also specific, because it was completely blocked by concomitant intrathecal injection of 1.6 μmol naloxone (Fig. 1*E*). In keeping with the distribution of δORs, as visualized by immunocytochemistry in a separate set of animals (Fig. 1*A*), specific binding and internalization of Fluo-DLT was detected in a subpopulation of small, medium, and large diameter DRG neurons (Fig. 1*B*). However, levels of internalized Fluo-DLT (i.e., fluorescence intensity per unit surface area) were higher in medium (Fig. 1*C*) and large (Fig. 1*D*) than in small (Fig. 1*C*) ganglion cells [1.33 ± 0.06 and 1.69 ± 0.09 for medium and large diameter neurons, respectively, vs 1.00 ± 0.04 for small diameter neurons; $p < 0.001$; one-way ANOVA followed by Bonferroni's multiple comparison test (MCT)] (see Fig. 3*B*, white columns).

To determine whether Fluo-DLT labeling of DRG neurons was caused by direct uptake of the ligand at the level of the ganglion or by its retrograde transport after presynaptic internalization at the level of the dorsal horn of the spinal cord, rats were injected intrathecally with 0.2 mg of colchicine 16 h before injection of Fluo-DLT. We first ascertained the efficacy of the treatment by comparing the distribution of β-tubulin immunostaining in saline-injected versus colchicine-treated rats. In control animals, β-tubulin-immunoreactive microtubules were evident throughout DRG axons (Fig. 2*A*). In contrast, in colchicine-treated rats, β-tubulin-immunoreactive microtubules were no longer evident (Fig. 2*B*). As shown in Table 1, colchicine treatment failed to significantly inhibit the accumulation of Fluo-DLT within ganglion cells, indicating that Fluo-DLT diffusing in the cerebrospinal fluid was internalized near, or at the level of DRG nerve cell bodies (two-tailed unpaired *t* test).

Effect of chronic morphine on cell surface δOR availability in whole DRGs and DRG neurons in culture

In vivo *internalization assay*

We demonstrated previously that chronic morphine-treatment resulted in increased Fluo-DLT internalization in neurons from the deeper laminas of the spinal cord (Morinville et al., 2004). To determine whether morphine similarly affected Fluo-DLT internalization in DRGs, rats were treated subcutaneously with increasing doses of morphine for 48 h (using doses of 5, 8, 10, and

15 mg/kg, respectively) and injected intrathecally with 0.8 nmol of Fluo-DLT. As shown in Figure 3, prolonged treatment with morphine induced a significant increase in the levels of internalized Fluo-DLT in all types of DRG neurons, compared with saline-treated animals ($p < 0.001$; two-tailed unpaired *t* test).

Real-time reverse transcriptase-PCR

To determine whether the morphine-induced increase in Fluo-DLT internalization was caused by an augmentation in the expression of δOR mRNA, real-time RT-PCR analysis was performed on mRNA extracts of DRG from saline- and morphine-treated animals. As seen in Table 2, δOR mRNA levels were not significantly different in ganglia from morphine-treated animals from those in saline-treated rats ($p > 0.05$; one-way ANOVA followed by Bonferroni's MCT), suggesting that the morphine-induced increase in Fluo-DLT internalization was caused by enhanced recruitment of reserve δORs to the cell surface rather than by an overall increase in receptor expression.

Electron microscopy

To demonstrate that the morphine-induced increase in Fluo-DLT internalization was indeed caused by perikaryal membrane recruitment of δORs, we quantified, by electron microscopic (EM) immunocytochemistry, the cell surface versus intracellular concentration of δORs after prolonged morphine exposure *in vivo* (in whole DRGs) and *in vitro* (in primary DRG cultures).

In DRG neurons labeled *in vivo*, gold particles indicative of δOR immunostaining were observed, as in light microscopic preparations, over small, medium, and large ganglion cells. The highest concentration of gold/silver particles (i.e., density of δOR immunostaining) was observed over type A_2 neurons, characterized as clear, large-diameter neurons in which evenly distributed Nissl bodies are separated from each other by pale wide strands of cytoplasm containing small stacks of Golgi saccules and rod-like mitochondria (Duce and Keen, 1977; Rambourg et al., 1983) (Fig. 4*A*). High densities of δOR immunostaining were also present over axon hillocks and unmyelinated axons (Fig. 4*B*). In both nerve cell bodies and axonal processes, δOR immunolabeling was predominantly intracellular and associated with a variety of membrane-bound organelles, including clear vesicles of various sizes and shapes, but hardly ever with large dense core vesicles (LDCVs). Only a small proportion of gold particles was detected over plasma membranes (Figs. 4*A*,*B*, insert and arrows, respectively). After prolonged exposure to morphine (48 h), there was a significant increase in the proportion of grains associated with plasma membranes (expressed as a percentage of the total number of grains detected within a depth of 1 μm from these membranes), compared with DRGs from saline-treated rats (21.9 ± 0.6% in DRGs from morphine-treated rats vs 13.9 ± 1.4% in DRGs from saline-treated animals; $p < 0.02$; χ^2 test).

Similarly, in DRG neurons grown in culture and exposed to 10 μM morphine for 48 h, the percentage of gold particles directly associated with neuronal plasma membranes was significantly increased over that observed in untreated cells (2.4 ± 0.6% in morphine-treated versus 0.6 ± 0.2% in untreated cells; $p < 0.01$; Kruskal–Wallis test followed by Dunn's MCT) (Fig. 5*A*). In contrast, there was no significant difference in δOR membrane densities before and after membrane depolarization with KCl (40 mM; 5 min; 0.3 ± 0.3%; $p > 0.05$; Kruskal–Wallis test followed by Dunn's MCT) (Fig. 5*A*). As in DRGs, δOR-like immunoreactivity in cultured neurons was only rarely associated with LDCVs (Fig. 5*B*; arrowheads indicate LDCVs and arrow points to δOR-like immunoreactivity associated with a LDCV).

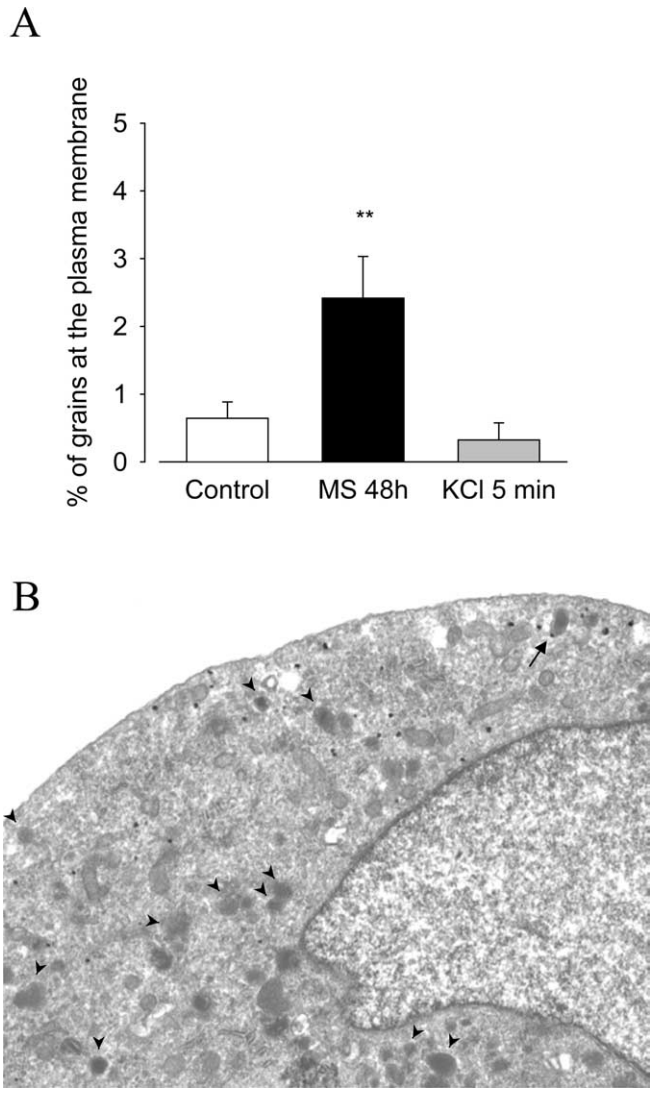

Figure 5. Effect of prolonged morphine treatment on the membrane targeting of δORs in cultured DRG neurons. DRG neurons where cultured as described in Material and Methods. Cells were left untreated (control) or were treated for either 48 h with 10 μM morphine or for 5 min with 40 mM KCl. ***A***, Morphine treatment for 48 h significantly increases the percentage of immunoreactive δORs found in direct contact with the plasma membrane, compared with control (**$p < 0.01$; Kruskal–Wallis test followed by Dunn's MCT). In contrast, KCl-induced membrane depolarization has no significant effect on δOR localization, compared with control ($p > 0.05$; Kruskal–Wallis test followed by Dunn's MCT). Data correspond to the mean ± SEM of the percentage of grains at the plasma membrane. ***B***, Within cultured DRG neurons, gold/silver grains are associated mainly with Nissl bodies and mitochondria but are only rarely found in association with LDCVs. Note that one grain is associated with a LDCV (arrow), whereas most LDCVs are not labeled with δOR antiserum (arrowheads).

Effect of chronic inflammation on cell surface δOR availability in DRGs

To determine whether chronic inflammation produced by injection of CFA into the hindpaw would also affect the bioavailability of δORs in dorsal root ganglion cells, internalization of intrathecally administered Fluo-DLT was visualized and quantified in DRGs 48 and 72 h after intraplantar CFA injection. We observed a significant increase in the levels of internalized Fluo-DLT in neuronal cell bodies from the ipsilateral DRGs in 72 h CFA-injected rats compared with naive rats (Figs. 6, 7). Most importantly, this increase was selective for small- and medium-sized DRG neurons (Figs. 6, 7). As after prolonged morphine treatment, these changes in Fluo-DLT internalization were not ac-

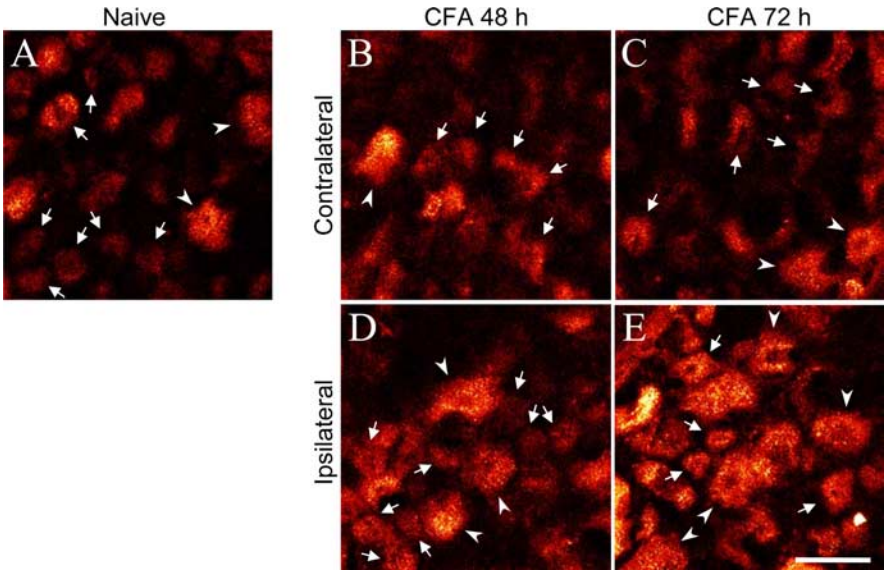

Figure 6. Effect of chronic inflammation on Fluo-DLT internalization in lumbar DRGs. ***A***, Rats were left untreated (naive) or were injected with 100 μl of CFA in the left hindpaw and maintained for 48 h (***B***, ***D***) or 72 h (***C***, ***E***). On the last day, they were injected intrathecally with 0.8 nmol of Fluo-DLT, and lumbar DRGs were processed for confocal microscopy as described. Seventy-two hours after CFA injection, levels of internalized Fluo-DLT are markedly increased in DRGs on the side ipsilateral to the injection (L4–L5 DRGs; red-white glow-scale images). Some small- and medium- (arrows) as well as large-diameter DRG neurons (arrowheads) are identified. Scale bar: (in ***E***) ***A–E***, 50 μm.

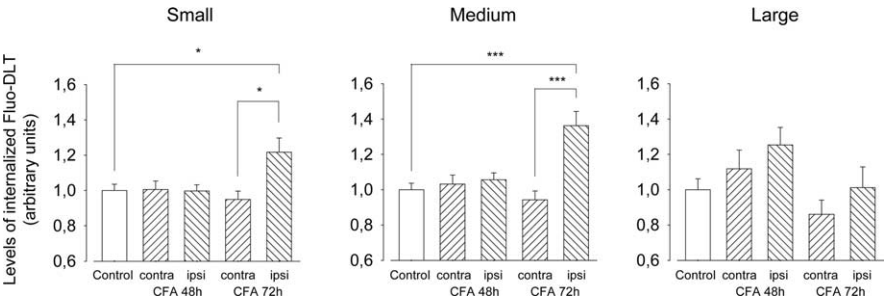

Figure 7. Densitometric analysis of the effect of chronic inflammation on Fluo-DLT internalization in L4–L5 DRGs. The levels of internalized Fluo-DLT in small, medium, and large DRG cell profiles were assessed in naive rats (white bars), as well as in rats injected 48 or 72 h earlier with CFA in the left hindpaw (hatched bars). Induction of chronic inflammatory pain by injection of CFA significantly increases the levels of internalized Fluo-DLT in small- and medium-sized DRG neurons on the side ipsilateral to the inflammation, 72 h after CFA injection. Data correspond to the levels of internalized Fluo-DLT ± SEM. Statistical significance was determined using one-way ANOVA followed by Bonferroni's multiple comparison test. *$p < 0.05$; ***$p < 0.001$.

companied by changes in δOR mRNA levels. Indeed, δORs mRNA levels measured by real-time PCR were not significantly different between DRGs from saline- and CFA-treated rats ($p > 0.05$; one-way ANOVA followed by Bonferroni's MCT) (Table 2).

Given the selectivity of CFA-induced changes in the levels of internalized Fluo-DLT for small- and medium-sized ganglion cells (i.e., for cells carrying primary nociceptive inputs), we hypothesized that these effects might be linked to pain-related stimulation of DRG neurons. To test this possibility, we injected 10 μl of a 0.5% capsaicin solution in the rat left hindpaw to selectively activate the subpopulation of nociceptive cells expressing the vanilloid/transient receptor potential vanilloid 1 (TRPV1) receptor. Fluo-DLT was injected via the lumbar puncture route exactly 1 h after injection of capsaicin. As shown in Figure 8, capsaicin injection in one hindpaw induced a selective increase in the levels of internalized Fluo-DLT within small-diameter neurons (identified by white arrows in each panel) in DRGs ipsilateral to the injection site compared with the contralateral side (51 ± 8% increase; $p < 0.001$; two-tailed unpaired *t* test) (Fig. 8*B–D*). In contrast, there was no significant difference between ipsilateral and contralateral sides in the amount of Fluo-DLT internalized within medium- and large-diameter neurons ($p > 0.05$; two-tailed unpaired *t* test) (Fig. 8*D*). Note that the levels of internalized Fluo-DLT in contralateral DRGs from capsaicin-injected animals (Fig. 8*B*) were similar to those in DRGs from untreated controls (Fig. 8*A*).

Discussion

The present results demonstrate that prolonged morphine treatment (48 h) and chronic inflammation (72 h) both promote externalization of δORs in rat dorsal root ganglion cells, thereby increasing local binding and internalization of intrathecally administered opioid drugs by these cells.

Previous *in situ* hybridization (Mansour et al., 1994; Minami et al., 1995; Zhang et al., 1998b; Wang and Wessendorf, 2001; Mennicken et al., 2003) and light microscopic immunohistochemical studies (Dado et al., 1993; Ji et al., 1995; Zhang et al., 1998b) have reported δORs to be expressed by small, medium, and large dorsal root ganglion cells of mouse, rat, monkey, and human DRGs. Immunohistochemical and autoradiographic studies also showed δORs to be associated with primary afferent fibers originating from DRGs and arborizing in the dorsal horn of the spinal cord (Goodman et al., 1980; Sharif and Hughes, 1989; Zajac et al., 1989; Besse et al., 1990, 1992; Dado et al., 1993; Arvidsson et al., 1995; Cheng et al., 1995; Ji et al., 1995; Zhang et al., 1998b; Robertson et al., 1999; Abbadie et al., 2002; Mennicken et al., 2003). Yet, δOR binding sites were not detected by autoradiography on the perikarya of DRG neurons, suggesting that δORs synthesized in the DRG might be entirely destined to spinally (or peripherally) projecting axons (Mennicken et al., 2003). Our electron microscopic data demonstrate that this is not the case because δOR immunoreactivity was observed at the surface as well as inside DRG nerve cell bodies. Admittedly, cell surface receptors were few in number, which probably explains the fact that they had escaped detection using classical autoradiographic receptor binding techniques (Mennicken et al., 2003).

Cell surface perikaryal δORs are functional because they were found here to bind and internalize the fluorescent deltorphin analog Fluo-DLT *in vivo*. Fluo-DLT labeling was specific in that it was completely abolished when the fluorescent ligand was coadministered with an excess of nonfluorescent naloxone. Also, the distribution of Fluo-DLT-labeled cells was similar to that of δOR-expressing neurons, as visualized by immunohistochemical and *in situ* hybridization techniques (Mansour et al., 1994; Wang and Wessendorf, 2001; Mennicken et al., 2003). Furthermore, the

densest accumulations of Fluo-DLT were observed over large ganglion cells, which were found by *in situ* hybridization to express the highest concentrations of δOR mRNA (Mansour et al., 1994; Mennicken et al., 2003). One could argue that the Fluo-DLT accumulation observed here at the level of DRG had, in fact, resulted from retrograde transport of Fluo-DLT molecules internalized by presynaptic afferent axons in the dorsal horn of the spinal cord. This was not the case, however, because rats injected intrathecally with colchicine, at doses shown previously to efficiently inhibit axonal transport (Hinkley and Green, 1971; Tohda et al., 2001; Lee et al., 2002) without affecting opioid receptor internalization (Lee et al., 2002), and found here to greatly reduce β-tubulin immunostaining, failed to show a significant difference in the intraperikaryal accumulation of Fluo-DLT.

Previous immunohistochemical studies have shown other G-protein-coupled receptors, including μOR (Ji et al., 1995; Zhang et al., 1998a) and neuropeptide Y Y1 receptors (Zhang et al., 1994, 1999; Shi et al., 1998), to be present on somatic plasma membranes of DRG neurons and to electrophysiologically respond to stimulation by peptide ligands *in vitro* (Zhang et al., 1994). However, the present study is the first to demonstrate that ganglionic somatic receptors may actually be accessed *in vivo* by intrathecally administered peptides and, thus, presumably also by endogenous peptides released in the CSF. Our results therefore suggest that intrathecally injected opioids may exert analgesic effects not only through their action at the level of the spinal cord, but also through direct, and selective, effects on DRG neurons.

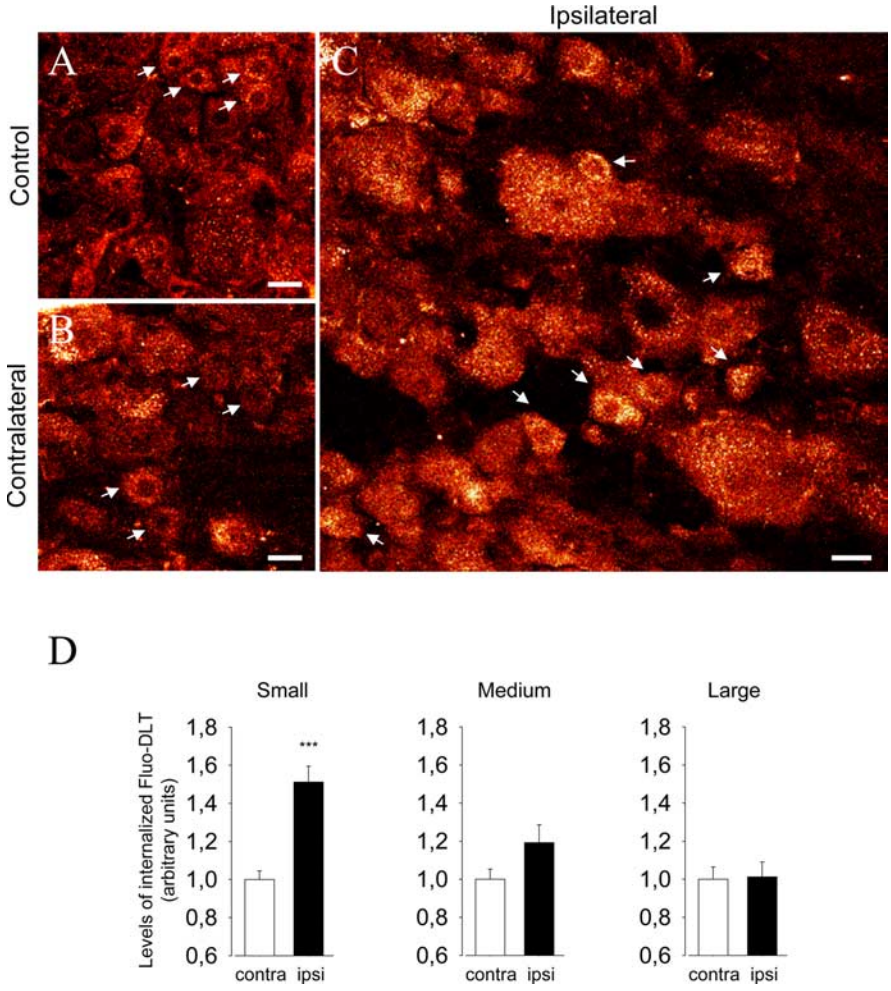

Figure 8. Effect of capsaicin injection on Fluo-DLT internalization in lumbar DRGs. Rats were injected subcutaneously with a 0.5% capsaicin solution (10 μl) in the plantar surface of the left hindpaw and were injected intrathecally 1 h later with 0.8 nmol of Fluo-DLT. Lumbar DRGs were then processed for confocal microscopy as described. ***A–C***, Red-white glow-scale images of L4–L5 DRGs from an untreated control animal (***A***) and the sides contralateral (***B***) and ipsilateral (***C***) to the capsaicin injection. ***D***, Levels of internalized Fluo-DLT in small, medium, and large DRG neurons after unilateral injection of capsaicin. Injection of capsaicin induces a selective increase of the levels of internalized Fluo-DLT in small-diameter DRG neurons on the side ipsilateral to the injection (***$p < 0.001$ when compared with the side contralateral of the injection; two-tailed unpaired *t* test). No significant difference is observed between contralateral (contra) and ipsilateral (ipsi) medium- and large-diameter neurons. Data correspond to the levels of internalized Fluo-DLT ± SEM. Small DRG neurons are identified by white arrows. Scale bars: ***A–C***, 20 μm.

Our previous studies on the rat spinal cord had demonstrated that the amount of internalized Fluo-DLT was tightly correlated with cell surface receptor density (Morinville et al., 2003). The increase in Fluo-DLT internalization observed here in DRG neurons of all sizes after prolonged morphine administration was, therefore, interpreted as reflecting enhanced δORs targeting to neuronal plasma membranes. Indeed, quantitative electron microscopic immunocytochemistry confirmed that prolonged morphine treatment induced an increase in the cell surface to intracellular receptor ratio after exposure to morphine *in vivo*. The absence of a significant difference in δOR mRNA levels between DRG of morphine- and saline-treated animals suggests that this increase is not related to enhanced δOR expression.

In spinal cord neurons, the morphine-induced increase in the membrane recruitment of δORs was shown to result from selective activation of μORs, because it was reproduced using selective μOR agonists and was abolished in the presence of the μOR antagonist D-Phe-Cys-Tyr-D-Trp-Orn-Thr-Pen-Thr-NH_2, as well as in μOR-KO mice (Morinville et al., 2003). The morphine-induced increase in the cell surface density of δORs observed here in DRGs likewise probably results from selective stimulation of μORs. The fact that a comparable increase in receptor density was detected here in DRG neurons in culture, coupled to the demonstrated expression of μORs by all DRG neuronal subtypes (Mansour et al., 1994; Ji et al., 1995; Minami et al., 1995; Wang and Wessendorf, 2001), further suggests that the observed cell surface upregulation of δORs results from μOR/δOR interactions within the same neurons.

Also consistent with our previous observations in the spinal cord (Cahill et al., 2003), CFA-induced chronic inflammatory pain also resulted in an increase in Fluo-DLT internalization in DRG neurons on the side ipsilateral to the CFA injection. However, unlike after sustained morphine, this increase was restricted to neurons of small and medium caliber. These small to medium DRG neurons are known to respectively give rise to C and Aδ fibers responsible for the transmission of noxious stimuli (for review, see Julius and Basbaum, 2001). This labeling selectivity suggested to us that the CFA-induced increase in the bioavailability of δORs could be attributable to modality-specific pain-

related neuronal stimulation. To investigate this possibility, we selectively stimulated nociceptive C fibers using intraplantar capsaicin, an agonist of TRPV1 receptors selectively expressed, under normal conditions, by these nociceptive axon terminals (Caterina et al., 1997; Michael and Priestley, 1999; Amaya et al., 2003). We found that capsaicin injections selectively increased Fluo-DLT internalization and, hence, cell surface δOR density in small DRG neurons, supporting our hypothesis of a modality-dependent δOR membrane targeting.

Previous studies have demonstrated an extensive association of δORs with LDCVs in DRG neurons and proposed that depolarization of these cells could lead to an externalization of δORs through vesicular exocytosis (van Bockstaele et al., 1997; Zhang et al., 1998b; Commons et al., 2001; Bao et al., 2003; Commons, 2003). Indeed, studies on DRG neurons in culture and PC12 cells reported an increase in the plasma membrane recruitment of δORs after neuronal depolarization with KCl (Bao et al., 2003; Kim and von Zastrow, 2003). In contrast, our own EM studies showed very little association between δORs and LDCVs, either *in vitro* or *in vivo*. Furthermore, we observed no significant cellular redistribution of δORs after application of KCl to cultured DRG neurons. In keeping with our observations, Hack et al. (2005) demonstrated recently that increasing extracellular potassium concentrations did not affect δOR-mediated presynaptic inhibition of GABAergic synaptic current in slices of periaqueductal gray. The increase in δOR cell surface density observed in chronic inflammatory pain conditions is therefore unlikely to be merely dependent on neuronal depolarization and exocytosis of LDCVs.

Together, the present results demonstrate that δORs present at the perikaryal surface of dorsal root ganglion cells are differentially upregulated by prolonged morphine treatment and chronic inflammation. Whereas the effects of the former are exerted on neurons of all sizes, most likely through selective and prolonged stimulation of μORs, those of the latter are restricted to neurons involved in the transmission of nociceptive inputs and appear to be linked to pain-related neuronal activation. Regardless of the mechanisms involved, these effects probably account, in part, for the enhanced antinociceptive efficacy of δ-selective agonists demonstrated after both sustained morphine and CFA treatments (Cahill et al., 2001, 2003; Morinville et al., 2003).

References

Abbadie C, Lombard MC, Besson JM, Trafton JA, Basbaum AI (2002) μ and δ opioid receptor-like immunoreactivity in the cervical spinal cord of the rat after dorsal rhizotomy or neonatal capsaicin: an analysis of pre- and postsynaptic receptor distributions. Brain Res 930:150–162.

Amaya F, Oh-hashi K, Naruse Y, Iijima N, Ueda M, Shimosato G, Tominaga M, Tanaka Y, Tanaka M (2003) Local inflammation increases vanilloid receptor 1 expression within distinct subgroups of DRG neurons. Brain Res 963:190–196.

Arvidsson U, Dado RJ, Riedl M, Lee JH, Law PY, Loh HH, Elde R, Wessendorf MW (1995) δ-Opioid receptor immunoreactivity: distribution in brainstem and spinal cord, and relationship to biogenic amines and enkephalin. J Neurosci 15:1215–1235.

Bao L, Jin SX, Zhang C, Wang LH, Xu ZZ, Zhang FX, Wang LC, Ning FS, Cai HJ, Guan JS, Xiao HS, Xu ZQ, He C, Hokfelt T, Zhou Z, Zhang X (2003) Activation of δ opioid receptors induces receptor insertion and neuropeptide secretion. Neuron 37:121–133.

Besse D, Lombard MC, Zajac JM, Roques BP, Besson JM (1990) Pre- and postsynaptic distribution of μ, δ, and κ opioid receptors in the superficial layers of the cervical dorsal horn of the rat spinal cord. Brain Res 521:15–22.

Besse D, Lombard MC, Perrot S, Besson JM (1992) Regulation of opioid binding sites in the superficial dorsal horn of the rat spinal cord following loose ligation of the sciatic nerve: comparison with sciatic nerve section and lumbar dorsal rhizotomy. Neuroscience 50:921–933.

Cahill CM, Morinville A, Lee MC, Vincent JP, Collier B, Beaudet A (2001) Prolonged morphine treatment targets δ opioid receptors to neuronal plasma membranes and enhances δ-mediated antinociception. J Neurosci 21:7598–7607.

Cahill CM, Morinville A, Hoffert C, O'Donnell D, Beaudet A (2003) Up-regulation and trafficking of δ opioid receptor in a model of chronic inflammation: implications for pain control. Pain 101:199–208.

Caterina MJ, Schumacher MA, Tominaga M, Rosen TA, Levine JD, Julius D (1997) The capsaicin receptor: a heat-activated ion channel in the pain pathway. Nature 389:816–824.

Cheng PY, Svingos AL, Wang H, Clarke CL, Jenab S, Beczkowska IW, Inturrisi CE, Pickel VM (1995) Ultrastructural immunolabeling shows prominent presynaptic vesicular localization of δ-opioid receptor within both enkephalin- and nonenkephalin-containing axon terminals in the superficial layers of the rat cervical spinal cord. J Neurosci 15:5976–5988.

Cheng PY, Liu-Chen LY, Pickel VM (1997) Dual ultrastructural immunocytochemical labeling of μ and δ opioid receptors in the superficial layers of the rat cervical spinal cord. Brain Res 778:367–380.

Colpaert FC (1996) System theory of pain and of opiate analgesia: no tolerance to opiates. Pharmacol Rev 48:355–402.

Commons KG (2003) Translocation of presynaptic δ opioid receptors in the ventrolateral periaqueductal gray after swim stress. J Comp Neurol 464:197–207.

Commons KG, Beck SG, Rudoy C, Van Bockstaele EJ (2001) Anatomical evidence for presynaptic modulation by the δ opioid receptor in the ventrolateral periaqueductal gray of the rat. J Comp Neurol 430:200–208.

Dado RJ, Law PY, Loh HH, Elde R (1993) Immunofluorescent identification of a δ (δ)-opioid receptor on primary afferent nerve terminals. NeuroReport 5:341–344.

Duce IR, Keen P (1977) An ultrastructural classification of the neuronal cell bodies of the rat dorsal root ganglion using zinc iodide-osmium impregnation. Cell Tissue Res 185:263–277.

Elde R, Arvidsson U, Riedl M, Vulchanova L, Lee JH, Dado R, Nakano A, Chakrabarti S, Zhang X, Loh HH (1995) Distribution of neuropeptide receptors. New views of peptidergic neurotransmission made possible by antibodies to opioid receptors. Ann NY Acad Sci 757:390–404.

Gendron L, Lucido AL, Mennicken F, O'Donnell D, Stroh T, Beaudet A (2004) Increased δ-opioid receptor internalization in rat dorsal root ganglia following prolonged morphine treatment or chronic inflammatory pain. Soc Neurosci Abstr 30:406.5.

Gendron L, Esdaile MJ, Vincent JP, Stroh T, Cahill CM, Beaudet A (2005) Morphine pre-treatment potentiates deltorphin anti-hyperalgesic efficacy in animals with chronic inflammatory pain. Soc Neurosci Abstr 31: 49.3.

Goodman RR, Snyder SH, Kuhar MJ, Young III WS (1980) Differentiation of δ and μ opiate receptor localizations by light microscopic autoradiography. Proc Natl Acad Sci USA 77:6239–6243.

Hack SP, Bagley EE, Chieng BC, Christie MJ (2005) Induction of δ-opioid receptor function in the midbrain after chronic morphine treatment. J Neurosci 25:3192–3198.

Hinkley Jr RE, Green LS (1971) Effects of halothane and colchicine on microtubules and electrical activity of rabbit vagus nerves. J Neurobiol 2:97–105.

Ji RR, Zhang Q, Law PY, Low HH, Elde R, Hokfelt T (1995) Expression of μ-, δ-, and κ-opioid receptor-like immunoreactivities in rat dorsal root ganglia after carrageenan-induced inflammation. J Neurosci 15:8156–8166.

Julius D, Basbaum AI (2001) Molecular mechanisms of nociception. Nature 413:203–210.

Kieffer BL (1999) Opioids: first lessons from knockout mice. Trends Pharmacol Sci 20:19–26.

Kim KA, von Zastrow M (2003) Neurotrophin-regulated sorting of opioid receptors in the biosynthetic pathway of neurosecretory cells. J Neurosci 23:2075–2085.

Kreek MJ (1996) Opioid receptors: some perspectives from early studies of their role in normal physiology, stress responsivity, and in specific addictive diseases. Neurochem Res 21:1469–1488.

Lee MC, Cahill CM, Vincent JP, Beaudet A (2002) Internalization and trafficking of opioid receptor ligands in rat cortical neurons. Synapse 43:102–111.

Mansour A, Fox CA, Burke S, Meng F, Thompson RC, Akil H, Watson SJ (1994) μ, δ, and κ opioid receptor mRNA expression in the rat CNS: an *in situ* hybridization study. J Comp Neurol 350:412–438.

May CN, Dashwood MR, Whitehead CJ, Mathias CJ (1989) Differential cardiovascular and respiratory responses to central administration of selective opioid agonists in conscious rabbits: correlation with receptor distribution. Br J Pharmacol 98:903–913.

Mennicken F, Zhang J, Hoffert C, Ahmad S, Beaudet A, O'Donnell D (2003) Phylogenetic changes in the expression of δ opioid receptors in spinal cord and dorsal root ganglia. J Comp Neurol 465:349–360.

Michael GJ, Priestley JV (1999) Differential expression of the mRNA for the vanilloid receptor subtype 1 in cells of the adult rat dorsal root and nodose ganglia and its downregulation by axotomy. J Neurosci 19:1844–1854.

Minami M, Maekawa K, Yabuuchi K, Satoh M (1995) Double *in situ* hybridization study on coexistence of μ-, δ- and κ-opioid receptor mRNAs with preprotachykinin A mRNA in the rat dorsal root ganglia. Brain Res Mol Brain Res 30:203–210.

Morinville A, Cahill CM, Esdaile MJ, Aibak H, Collier B, Kieffer BL, Beaudet A (2003) Regulation of δ-opioid receptor trafficking via μ-opioid receptor stimulation: evidence from μ-opioid receptor knock-out mice. J Neurosci 23:4888–4898.

Morinville A, Cahill CM, Aibak H, Rymar VV, Pradhan A, Hoffert C, Mennicken F, Stroh T, Sadikot AF, O'Donnell D, Clarke PB, Collier B, Henry JL, Vincent JP, Beaudet A (2004) Morphine-induced changes in δ opioid receptor trafficking are linked to somatosensory processing in the rat spinal cord. J Neurosci 24:5549–5559.

Petrillo P, Angelici O, Bingham S, Ficalora G, Garnier M, Zaratin PF, Petrone G, Pozzi O, Sbacchi M, Stean TO, Upton N, Dondio GM, Scheideler MA (2003) Evidence for a selective role of the δ-opioid agonist [8*R*-(4bS*,8aα,8aβ, 12bβ)]7,10-dimethyl-1-methoxy-11-(2-methylpropyl) oxycarbonyl 5,6,7,8,12,12b-hexahydro-(9*H*)-4,8-methanobenzofuro [3,2-e]pyrrolo[2,3-g]iso quinoline hydrochloride (SB-235863) in blocking hyperalgesia associated with inflammatory and neuropathic pain responses. J Pharmacol Exp Ther 307:1079–1089.

Porreca F, Mosberg HI, Hurst R, Hruby VJ, Burks TF (1984) Roles of μ, δ and κ opioid receptors in spinal and supraspinal mediation of gastrointestinal transit effects and hot-plate analgesia in the mouse. J Pharmacol Exp Ther 230:341–348.

Rambourg A, Clermont Y, Beaudet A (1983) Ultrastructural features of six types of neurons in rat dorsal root ganglia. J Neurocytol 12:47–66.

Robertson B, Schulte G, Elde R, Grant G (1999) Effects of sciatic nerve injuries on δ-opioid receptor and substance P immunoreactivities in the superficial dorsal horn of the rat. Eur J Pain 3:115–129.

Sharif NA, Hughes J (1989) Discrete mapping of brain μ and δ opioid receptors using selective peptides: quantitative autoradiography, species differences and comparison with κ receptors. Peptides 10:499–522.

Sheldon RJ, Riviere PJ, Malarchik ME, Moseberg HI, Burks TF, Porreca F (1990) Opioid regulation of mucosal ion transport in the mouse isolated jejunum. J Pharmacol Exp Ther 253:144–151.

Shi TJ, Zhang X, Berge OG, Erickson JC, Palmiter RD, Hokfelt T (1998) Effect of peripheral axotomy on dorsal root ganglion neuron phenotype and autonomy behaviour in neuropeptide Y-deficient mice. Regul Pept 75- 76:161–173.

Stewart PE, Hammond DL (1994) Activation of spinal δ-1 or δ-2 opioid receptors reduces carrageenan-induced hyperalgesia in the rat. J Pharmacol Exp Ther 268:701–708.

Szeto HH, Soong Y, Wu D, Olariu N, Kett A, Kim H, Clapp JF (1999) Respiratory depression after intravenous administration of δ-selective opioid peptide analogs. Peptides 20:101–105.

Tohda C, Sasaki M, Konemura T, Sasamura T, Itoh M, Kuraishi Y (2001) Axonal transport of VR1 capsaicin receptor mRNA in primary afferents and its participation in inflammation-induced increase in capsaicin sensitivity. J Neurochem 76:1628–1635.

van Bockstaele EJ, Commons K, Pickel VM (1997) δ-Opioid receptor is present in presynaptic axon terminals in the rat nucleus locus coeruleus: relationships with methionine5-enkephalin. J Comp Neurol 388:575–586.

Wang H, Wessendorf MW (2001) Equal proportions of small and large DRG neurons express opioid receptor mRNAs. J Comp Neurol 429:590–600.

Zajac JM, Lombard MC, Peschanski M, Besson JM, Roques BP (1989) Autoradiographic study of μ and δ opioid binding sites and neutral endopeptidase-24.11 in rat after dorsal root rhizotomy. Brain Res 477:400–403.

Zhang X, Bao L, Xu ZQ, Kopp J, Arvidsson U, Elde R, Hokfelt T (1994) Localization of neuropeptide Y Y1 receptors in the rat nervous system with special reference to somatic receptors on small dorsal root ganglion neurons. Proc Natl Acad Sci USA 91:11738–11742.

Zhang X, Bao L, Shi TJ, Ju G, Elde R, Hokfelt T (1998a) Down-regulation of μ-opioid receptors in rat and monkey dorsal root ganglion neurons and spinal cord after peripheral axotomy. Neuroscience 82:223–240.

Zhang X, Bao L, Arvidsson U, Elde R, Hokfelt T (1998b) Localization and regulation of the δ-opioid receptor in dorsal root ganglia and spinal cord of the rat and monkey: evidence for association with the membrane of large dense-core vesicles. Neuroscience 82:1225–1242.

Zhang X, Tong YG, Bao L, Hokfelt T (1999) The neuropeptide Y Y1 receptor is a somatic receptor on dorsal root ganglion neurons and a postsynaptic receptor on somatostatin dorsal horn neurons. Eur J Neurosci 11:2211–2225.